

# Phase diagram of the semimetal graphite in the magnetic ultra-quantum limit

F. Arnold,<sup>1</sup> A. Isidori,<sup>1</sup> E. Kampert,<sup>2</sup> B. Yager,<sup>1</sup> M. Eschrig,<sup>1</sup> and J. Saunders<sup>1</sup>

<sup>1</sup>Royal Holloway, University of London, TW20 0EX Egham, United Kingdom

<sup>2</sup>Hochfeld-Magnetlabor Dresden (HLD), Helmholtz-Zentrum Dresden-Rossendorf, D-01328 Dresden, Germany  
(Dated: November 15, 2021)

Strong correlations within the lowest Landau levels of semimetals in their ultra-quantum limit give rise to collective phenomena and topologically non-trivial states. Using state-of-the-art pulsed magnetic fields up to 60 T applied to a high-quality single crystal of graphite, we find a series of field-induced transitions into collinear charge-density wave states. Our analysis establishes the phase diagram of graphite in its ultra-quantum limit. The results imply the existence of a novel topologically-protected chiral edge state at high fields, supporting both charge and spin currents.

Three-dimensional semimetals are of particular interest as their low charge carrier density gives rise to a rich variety of magnetic field driven collective and topological quantum phases [1–5]. For most conventional metals the topologically non-trivial quantum Hall regime, dominated by Landau level quantization, is far beyond reach due to the extraordinarily high magnetic fields required. However, in semimetals like bismuth and graphite, the ultra-quantum limit can be realised in state-of-the-art high-magnetic field laboratories. In the quantum limit, interactions between the lowest Landau levels are enhanced by nesting, leading to the possibility of field-induced spin- and charge-density wave instabilities (SDWs and CDWs, respectively) with ordering wave vector along the field direction. Similarly to one-dimensional electron gases, which are unstable toward the formation of SDWs [6], any three-dimensional electron gas in a sufficiently strong magnetic field, or with large parallel sections of the Fermi surface, is prone to density wave instabilities [1, 7, 8].

Graphite is a well known three-dimensional semimetal with a large Fermi-surface anisotropy which can be viewed as an infinite number of stacked graphene sheets [9, 10]. The zero-field band structure of graphite is well described by the tight-binding Slonczewski-Weiss-McClure model [11–14]. The Fermi surface consists of trigonally warped ellipsoidal electron and hole pockets located along the H-K-H and H'-K'-H' edges of the hexagonal Brillouin zone (see Fig. 1). In magnetic fields applied perpendicular to the graphene layers, the  $E_3$ -band, which is slightly hybridised with the  $E_1$  and  $E_2$  bands in proximity of the H points, gives rise to two one-dimensional Landau levels (LLs) with LL-index  $n = -1$  and  $n = 0$ . Each LL is spin-split by the Zeeman energy and has a residual twofold valley-degeneracy associated with the two inequivalent H-K-H and H'-K'-H' edges. For magnetic fields above 8 T these are the only LLs that cross the Fermi energy. In this regime the system becomes effectively quasi-one-dimensional, entering the so-called magnetic ultra-quantum limit. The field-induced dimensional reduction strongly enhances electronic correlations, leading to Luttinger liquid [15] properties such as logarithmic

nesting singularities in the response functions and the consequent tendency towards formation of density-wave ordered phases.

The first magneto-transport measurements by Iye *et al.* on Kish graphite showed a pronounced resistance anomaly above 22 T [16]. Nakao [17], Yoshioka and Fukuyama [18] attributed the observed resistance anomaly to the formation of a CDW in the lower LLs and developed a mean-field theory describing the magnetic field dependence of its critical temperature. Subsequent experiments by Iye and Yaguchi *et al.* [19–21] up to higher fields identified a series of other possible transitions, observing the collapse of the putative CDW-phase at 52 T. More recently, Fauqué *et al.* [22] showed the evolution of a second density-wave anomaly above 53 T by out-of-plane transport measurements on Kish graphite up to 80 T. Despite improved LL calculations by Takada and Goto [23], attempts to directly measure the density-wave gap spectroscopically [24, 25], and the discovery of a second density-wave anomaly above 53 T, the precise nature of the magnetic field driven density-wave states has remained unclear. Different scenarios for possible nestings within the hole-like  $n = -1$  and electron-like  $n = 0$  LLs have been proposed, trying to explain the observed resistance anomalies in terms of SDWs and CDWs, but

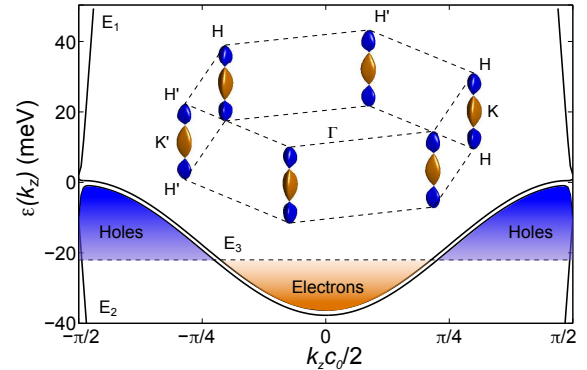


Figure 1. Zero-field  $k_z$ -dependence of graphite's band structure along the H-K-H and H'-K'-H' edges of the hexagonal Brillouin zone.

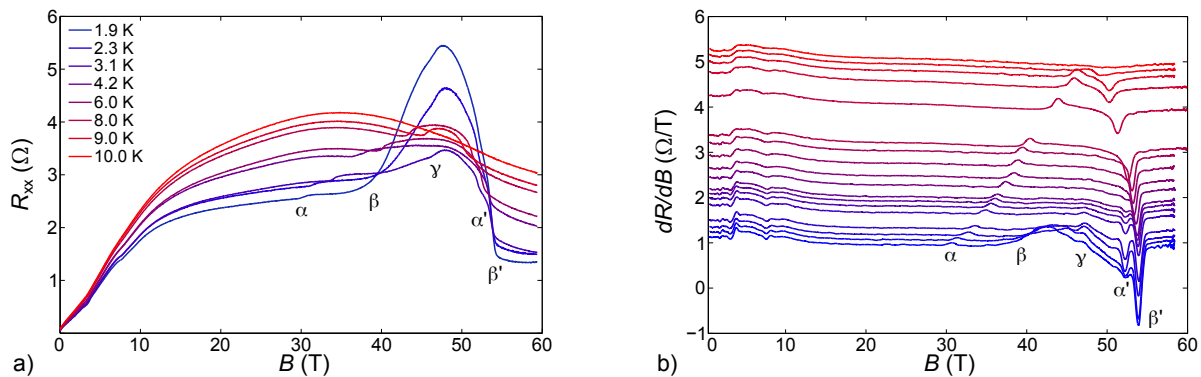


Figure 2. a) Magnetic field dependence of the in-plane resistance of graphite for temperatures below 10 K measured in a 25 ms 60 T pulsed field magnet. b) Magnetic field derivatives of the in-plane resistance at temperatures below 10 K. The data in b) has been offset proportional to the temperature by  $0.5 \Omega = TK$  for clarity.  $\alpha$  and  $\beta$  denote the onset transitions of the CDWs in the  $(0; \uparrow)$  and  $(-1; \downarrow)$ , whereas  $\alpha'$  and  $\beta'$  mark the field at which they vanish. At  $\alpha'$  the CDW associated with the  $(0; \uparrow)$  LL undergoes a lock-in transition.

none of them succeeded in finding a conclusive explanation.

In this article we present decisive theoretical and experimental evidence that enables to identify the observed resistance anomalies with the formation of CDWs in specific LLs. We discovered new features in the magnetotransport which allows us to track the onset and subsequent disappearance of density-wave instabilities in two distinct LLs. We show that the resistance anomaly below 54.2 T, contrary to previous reports, is a superposition state of two incommensurate collinear CDWs with different onset and vanishing fields. One of these undergoes a lock-in transition at 47.1 T before both CDWs vanish due to the emptying of their corresponding LLs at 52.3 and 54.2 T respectively. The observation of a third resistance anomaly, together with our refined LL calculations, rules out any transverse-SDW and excitonic-insulator scenarios. In addition, we discuss the implications of our calculations on the upper CDW-phase [22] and the magnetotransport properties in the ultra-quantum limit.

We performed electrical transport measurements on a single crystal of Tanzanian natural graphite [26], the quality of which significantly exceeds the commonly used Kish graphite, highly-oriented-pyrolytic graphite, or other natural graphites. Pulsed magnetic fields up to 60 T were applied to bring the system into the ultra-quantum limit [27, 28].

Figure 2 shows the in-plane resistance of the graphite crystal for fields up to 60 T and temperatures below 10 K. The in-plane resistance first increases steeply, superimposed by Shubnikov-de Haas oscillations. Above 15 T it saturates due to the so-called magnetic freeze-out, i.e., charge carrier localization in high magnetic field [1, 16, 29, 30]. In this field range the band-structure of graphite becomes quasi-one-dimensional along the magnetic field direction and is thus susceptible to CDW and SDW instabilities. At lowest temperatures a step is ob-

served in the in-plane resistance at around 30 T, followed by a steep increase of the resistance, reaching its maximum value at 48 T before it drops down to below its initial value at around 53 T. This behavior has already been reported for Kish and highly-oriented-pyrolytic graphite and has been attributed to the formation of a CDW state [16, 19–22]. Similar features can also be identified in the out-of plane transport [22, 28].

In order to reveal and precisely identify the transitions in our sample, the magnetic field derivatives of the in-plane magnetoresistance were calculated (see Fig. 2). Here the transitions appear as maxima and minima. We denote the observed maxima as  $\alpha$ ,  $\beta$ , and  $\gamma$ , in ascending order of their transition fields, and the corresponding minima as  $\alpha'$  and  $\beta'$ . In addition to the well known  $\alpha$ ,  $\beta$ , and  $\alpha'$ , we find two more phase transitions named  $\gamma$  and  $\beta'$ . The  $\gamma$ -transition around  $47.1 \pm 0.1$  T can only be observed below 3 K and represents another step resistance increase, whereas the  $\beta'$  transition develops below 6 K alongside the  $\alpha'$  transition. Both of these phase transitions are essentially temperature independent. We find that  $\alpha$ ,  $\gamma$ ,  $\alpha'$ , and  $\beta'$ , are sharp step-like transitions, whereas  $\beta$  is a much less well-defined transition. We thus define a more precise value for  $\beta$  as the extrapolated crossing field of the two linear resistive regimes either side of the transition rather than using the derivative maxima. The temperature dependence of all these transitions is shown in the phase diagram of Fig. 5.

Inspired by Takada and Goto's calculations [23], we decided to investigate more closely the magnetic field dependence of the putative nesting vectors in all the four LLs that are close to the Fermi level in the ultra-quantum limit (see Fig. 3). Since in this regime the system becomes effectively one-dimensional, electron correlations play a significant role in renormalizing the bare Slonczewski-Weiss-McClure LL structure. We therefore calculate the renormalized LLs by including the electron

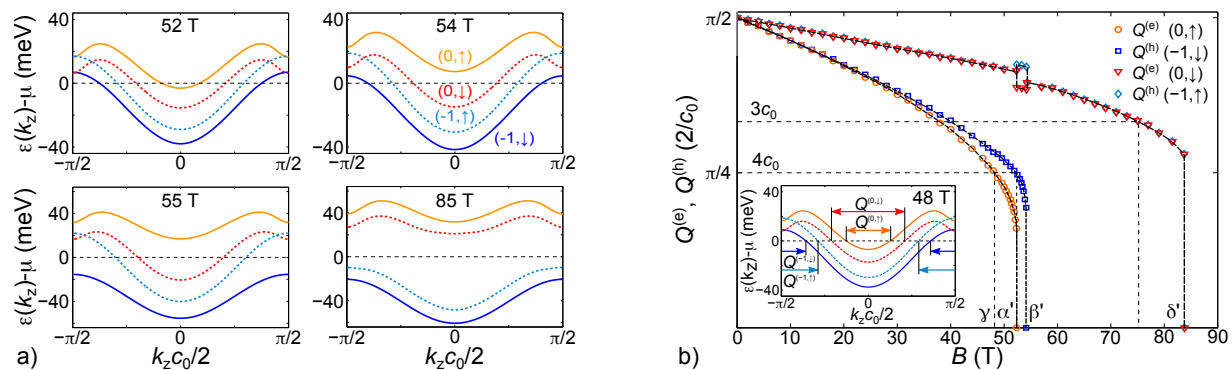


Figure 3. a) Renormalized LL structure in the ultra-quantum limit: Above 8 T only the lowest four LLs cross the Fermi energy. b) CDW nesting vectors up to 90 T. The nesting vectors of the hole-like  $(-1; \downarrow)$  LLs are given by  $Q^{(h)} = 2k_F^{(h)} = 2\pi/c_0 - 2k_F$  (see inset). The CDW nesting vectors decrease with increasing magnetic field due to the upward and downward shift of the electron-like  $(0; \downarrow)$  and hole-like  $(-1; \downarrow)$  LLs, before vanishing in a first-order transition at  $B_{\alpha'} = 52.3$  T,  $B_{\beta'} = 54.2$  T, and  $B_{\delta'} = 84$  T. The nesting vector of the  $(0; \uparrow)$  LL becomes commensurate at around  $B_\gamma = 48$  T.

self-energy in a fully self-consistent manner [28]. The effect of short-range correlations, neglected by the conventional random-phase approximation (RPA), is included via the so-called local-field correction [31, 32] to the effective electron-electron interaction.

At  $B_\gamma = 48$  T our calculation predicts that the nesting vector  $Q^{(0,\uparrow)} = 2k_F^{(0,\uparrow)}$  of the  $(0, \uparrow)$  LL takes the value of  $2\pi/4c_0$ , corresponding to a commensurate wavelength of  $4c_0$ , where  $c_0/2$  is the distance between adjacent graphene layers (see Fig. 3). This suggests that the temperature-independent  $\gamma$ -transition, observed experimentally at 47.1 T (see Fig. 2), is a lock-in transition of the corresponding LL.

Increasing the magnetic field, at  $B_{\alpha'} = 52.3 \pm 0.1$  T the bottom of the  $(0, \uparrow)$  electron-like level crosses the Fermi energy (see Fig. 3). The abrupt depopulation of the LL determines the sudden collapse of the associated CDW order, resulting in a first-order, almost temperature-independent transition (see Fig. 4 and 5). In our calculation we use the experimental value of  $B_{\alpha'}$  to fix the only free-parameter that appears in our theory [28]. The first-order character of the transition, predicted by our theory, is experimentally confirmed by the clear evidence of hysteresis, as shown in Fig. 4. On the other hand, the nesting vector of the  $(-1, \downarrow)$  hole-like level,  $Q^{(-1,\downarrow)} = 2\pi/c_0 - 2k_F^{(-1,\downarrow)}$ , remains finite across the  $\alpha'$  transition, so that the corresponding CDW ordered state persists. In this magnetic field region only two hole- and one electron-like LLs are present at the Fermi level. These three levels must therefore adjust their Fermi-wave vectors to guarantee the imposed charge balance, leading to the splitting of the Fermi-wave vectors of the  $(0, \downarrow)$  and  $(-1, \uparrow)$  bands (see Fig. 3). In our calculation the hole-like nesting vector  $Q^{(-1,\downarrow)}$  vanishes also with a first-order transition at  $B_{\beta'} = 54.2$  T, in remarkable agreement with the observed experimental value of  $54.2 \pm 0.1$  T. As for the previous transition, the CDW order is destroyed by

the sudden depopulation of the corresponding LL. Note the larger discontinuity of the  $Q^{(-1,\downarrow)}$  vector, in comparison to  $Q^{(0,\uparrow)}$ , resulting in the larger hysteresis loop observed experimentally (see Fig. 4). The resistance hysteresis around  $\alpha'$  and  $\beta'$  was already observed by Yaguchi *et al.* [33]. However, due to a presumably lower sample quality and higher field sweep rates in their experiment, a distinction between the two first order transitions was not possible.

The slight difference in the critical-field values of the  $\alpha'$  and  $\beta'$  transitions, emerging both from the experimental observation and theoretical prediction, makes it possible for the first time to attribute the experimentally observed phases to Fermi-level nesting within the  $(0, \uparrow)$  and  $(-1, \downarrow)$  bands (see Fig. 5). This finding, in conjunction with the observation of another density-wave instability above 54.2 T [22], rules out the possibility of a transverse SDW order, which would couple the up-spin and down-spin energy levels. In fact, if the first putative SDW-state coupled the  $(0, \uparrow)$  and  $(-1, \downarrow)$  levels (with the possibility of a second SDW-state coupling the remaining two levels above 54.2 T), the first SDW phase would disappear with a single first-order transition at the field value corresponding to the  $\alpha'$ -transition, in contrast with the two distinct transitions ( $\alpha'$  and  $\beta'$ ) observed around 53 T. If, instead, the SDW nesting vectors were coupling the  $(0, \uparrow)$  and  $(0, \downarrow)$  levels on the one hand, and the  $(-1, \uparrow)$  and  $(-1, \downarrow)$  levels on the other, then there would be no possibility of another density-wave instability to form above 54.2 T. The very existence of at least three distinct density-wave instabilities thus leads to the identification of such instabilities as CDW ordered states. We also point out that the observation of a second CDW-state below 54.2 T contradicts the LL structures proposed by Fauqué *et al.* [22].

For magnetic fields above  $\beta'$  the populated LLs are  $(0, \downarrow)$  and  $(-1, \uparrow)$ . These LLs are still characterized by fi-

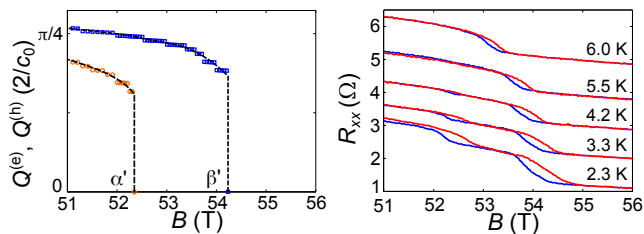


Figure 4. a) Close-up of the nesting vectors in the vicinity of the first-order transitions in the  $(0; \uparrow)$  and  $(-1; \downarrow)$  LLs around 52.3 and 54.2 T. b) Observed resistance hysteresis around the first-order  $\alpha'$  and  $\beta'$ -transitions: The red curves show the magnetic field up-sweeps whereas the blue curves correspond to the down-sweeps.

nite nesting vectors until both levels become depopulated of carriers at 84 T. The nesting vectors arising from these bands are almost identical due to the imposed charge balance. Both nesting vectors could give rise to additional lock-in transitions due to their commensuration with a wavelength of  $3c_0$  around 75 T. Above  $B_{\delta'} = 84$  T we predict that graphite becomes insulating, with a vanishing carrier density in the bulk. The origin of quantitative discrepancies in the observed upper critical fields of Fauqué *et al.* ( $B_{\delta'} = 75$  T) [22] and our calculations ( $B_{\delta'} = 84$  T) is unresolved.

In summary we have identified the CDW instabilities in the LLs responsible for the magnetic field driven resistance anomalies in the in- and out-of-plane resistance of graphite. We showed experimentally and theoretically that the lower resistance anomaly in graphite is generated by two collinear CDWs in the  $(0, \uparrow)$  and  $(-1, \downarrow)$  LLs. The observed  $\gamma$ ,  $\alpha'$  and  $\beta'$ -transitions at 47.1, 52.3 and 54.2 T can be explained by a lock-in transition of the  $(0, \uparrow)$  CDW and emptying of the  $(0, \uparrow)$  and  $(-1, \downarrow)$  LLs respectively. At 47.1 T the nesting vector of the  $(0, \uparrow)$  LL becomes commensurate with a wavelength of  $4c_0$ . At 52.3 T the nesting vector of the electron-like  $(0, \uparrow)$  level vanishes with a first-order transition, followed by another first-order transition at 54.2 T when the hole-like  $(-1, \downarrow)$  level becomes depopulated. Above 54.2 T graphite develops a third CDW state in the remaining  $(0, \downarrow)$  and  $(-1, \uparrow)$  LLs whose nesting vectors become commensurate with a wavelength of  $3c_0$  before both LLs get emptied with a first-order transition.

In addition, we discuss the implications of this analysis on our understanding of undoped graphite in the ultra-quantum limit. Above the onset transition for the CDW in the  $(0, \downarrow)$  and  $(-1, \uparrow)$ , the bulk LLs are gapped and graphite becomes in all respects a topological insulator, namely a three-dimensional quantum Hall system with filling factor  $\nu = 1$  [1, 34]. In this magnetic field regime our results imply the appearance of chiral surface states, supporting both spin and charge currents, which dominate the low-temperature transport properties [35, 36].

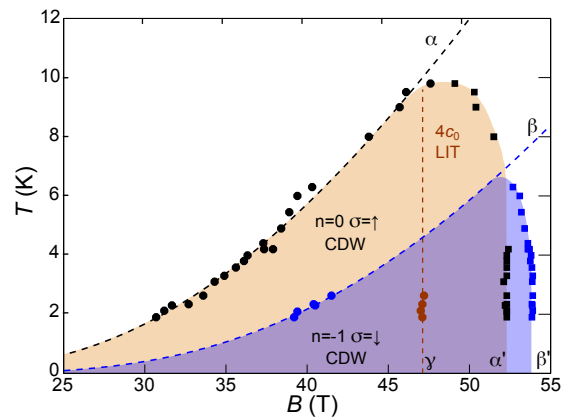


Figure 5. Phase diagram of the CDWs in the  $(0; \uparrow)$  and  $(-1; \downarrow)$  LLs. Circles and squares are phase transitions with a positive and negative differential magnetoresistance, respectively, where black represents the  $\alpha$ , blue the  $\beta$ , and orange the  $\gamma$ -transitions. At low fields the critical temperature of  $\alpha$  and  $\beta$  increases exponentially according to the Yoshioka-Fukuyama theory [18] (black and blue dashed lines):  $T_c(B) = T^* \exp\{-B^*/B\}$ , with  $T_\alpha^* = 230$  K,  $B_\alpha^* = 148$  T,  $T_\beta^* = 300$  K,  $B_\beta^* = 195$  T.

For fields above 84 T our LL structure predicts fully gapped bulk states, with edge currents arising from the upward shift, on approaching the sample edge, of the hole-like  $(-1, \downarrow)$  and  $(-1, \uparrow)$   $k_z$ -LL dispersions. Besides charge currents, spin currents arise due to the energy splitting of the spin-up and spin-down hole-like levels, with the consequent different penetration length of the corresponding edge states.

The chiral nature of these edge states leads to ballistic transport perpendicular to the magnetic field, whereas the transport along the magnetic field is governed by interlayer hopping and remains diffusive [35, 37]. In this regime we therefore expect that any changes to the bulk LL-structure are only observable in the out-of-plane transport and are absent in the in-plane transport, accounting for the absence of the CDW-signature in the in-plane resistance (Fig. 2) above 54.2 T.

On the other hand, below 54.2 T we expect transport to be governed both by bulk and surface states, and the situation is more complex, involving hybridization of bulk and surface states, as well as a strong dependence on impurity scattering. At lower magnetic fields, for example, the absence of the  $\alpha$ -signature in the out-of-plane resistance [37] still remains unclear.

Direct exploration of these novel chiral edge states in the ultra-quantum limit would be of great interest, as well as studies of the influence of stacking defects, twist, and modifications to the  $c$ -axis dispersion by intercalation.

The authors wish to thank T. Förster, J. Law, J. Wosnitza, T. Herrmansdörfer and S. Zherlitsyn for experimental support at the HLD. We acknowledge the support of the HLD-HZDR, member of the European Magnetic

Field Laboratory (EMFL) as well as the Hubbard Theory Consortium and Engineering and Physical Science Research Council (EPSRC Grant Nos. EP/H048375/1 and EP/J010618/1).

- 
- [1] B. I. Halperin, *Jap. J. Appl. Phys.* **26**, 1913 (1987).
- [2] K. Behnia, L. Balicas, and Y. Kopelevich, *Science* **317**, 1729 (2007).
- [3] A. Banerjee, B. Fauqué, K. Izawa, A. Miyake, I. Sheikin, J. Flouquet, B. Lenoir, and K. Behnia, *Phys. Rev. B* **78**, 161103(R) (2008).
- [4] H. Yang, B. Fauqué, L. Malone, A. Antunes, Z. Zhu, C. Uher, and K. Behnia, *Nature Comms.* **1** (2010).
- [5] J. Alicea, Unexpected richness in the high-field physics of graphite, Comment on [22] published in the Journal Club for Condensed Matter Physics JCCM-AUGUST-2014-01.
- [6] A. W. Overhauser, *Phys. Rev. Lett.* **4**, 462 (1960).
- [7] A. W. Overhauser, *Phys. Rev.* **167**, 691 (1968).
- [8] V. Celli and N. D. Mermin, *Phys. Rev.* **140**, A839 (1965).
- [9] K. Novoselov, A. Geim, S. Morozov, M. Katsnelson, I. Grigorieva, S. Dubonos, and A. Firsov, *Nature* **438**, 197 (2005).
- [10] A. Castro-Neto, F. Guinea, N. Peres, K. Novoselov, and A. Geim, *Rev. Mod. Phys.* **81**, 109 (2009).
- [11] P. R. Wallace, *Phys. Rev.* **71**, 622 (1946).
- [12] J. W. McClure, *Phys. Rev.* **108**, 612 (1957).
- [13] J. C. Slonczewski and P. R. Weiss, *Phys. Rev.* **109**, 272 (1958).
- [14] J. W. McClure, *Phys. Rev.* **119**, 606 (1960).
- [15] C. Biagini, D. L. Maslov, M. Y. Reizer, and L. I. Glazman, *Europhys. Lett.* **55**, 383 (2001).
- [16] Y. Iye, P. M. Tedrow, G. Timp, M. Shayegan, M. S. Dresselhaus, G. Dresselhaus, A. Furukawa, and S. Tanuma, *Phys. Rev. B* **25**, 5478 (1982).
- [17] K. Nakao, *J. Phys. Soc. Jpn.* **40**, 761 (1976).
- [18] D. Yoshioka and H. Fukuyama, *J. Phys. Soc. Japan* **50**, 725 (1981).
- [19] H. Yaguchi, Y. Iye, T. Takamasu, and N. Miura, *Physica B* **184**, 332 (1993).
- [20] S. Uji, J. Brooks, and Y. Iye, *Physica B* **246-247**, 299 (1998).
- [21] H. Yaguchi and J. Singleton, *J. Phys.: Condens. Matter* **21**, 344207 (2009).
- [22] B. Fauqué, D. LeBoeuf, B. Vignolle, M. Nardone, C. Proust, and K. Behnia, *Phys. Rev. Lett.* **110**, 266601 (2013).
- [23] Y. Takada and H. Goto, *J. Phys.: Condens. Matter* **10**, 11315 (1998).
- [24] Y. I. Latyshev, A. P. Orlov, D. Vignolles, W. Escoffier, and P. Monceau, *Physica B* **407**, 1885 (2012).
- [25] F. Arnold, B. Yager, E. Kamper, C. Putzke, J. Nyéki, and J. Saunders, *Rev. Sci. Instr.* **84**, 113901 (2013).
- [26] Naturally Graphite, Nanotech Innovations, Michigan Technological University, 1400 Townsend Drive, Houghton, Michigan 49931-1295, United States.
- [27] S. Zherlitsyn, T. Herrmannsdörfer, B. Wustmann, and J. Wosnitzer, *IEEE Trans. Appl. Supercon.* **20**, 672 (2010).
- [28] See Supplemental Material at URL for experimental and theoretical details.
- [29] N. B. Brandt, G. A. Kapustin, V. G. Karavaev, A. S. Kotosonov, and E. A. Svistova, *Sov. Phys.-JETP* **40**, 564 (1975).
- [30] K. Sugihara and J. A. Woollam, *J. Phys. Soc. Jpn.* **45**, 1891 (1978).
- [31] J. Hubbard, *Proc. R. Soc. Lond. A* **243**, 336 (1958).
- [32] K. S. Singwi, M. P. Tosi, R. H. Land, and A. Sjölander, *Phys. Rev.* **176**, 589 (1968).
- [33] H. Yaguchi, M. Tokunaga, A. Matsuo, and K. Kindo, “Exploration of the multiple field induced density wave phase in graphite using 75-t-class pulsed magnetic fields,” (2013), poster presented at the Strongly Correlated Electron Systems Conference, Aug. 5–9 2013, Tokyo, Japan.
- [34] B. I. Halperin, *Phys. Rev. B* **25**, 2185 (1982).
- [35] L. Balents and M. P. A. Fisher, *Phys. Rev. Lett.* **76**, 2782 (1996).
- [36] A. F. Young, J. D. Sanchez-Yamagishi, B. Hunt, S. H. Choi, K. Watanabe, T. Taniguchi, R. C. Ashoori, and P. Jarillo-Herrero, *Nature* **505**, 528 (2014).
- [37] S. Cho, L. Balents, and M. P. A. Fisher, *Phys. Rev. B* **56**, 15814 (1997).